Eur. Phys. J. B **18**, 63–66 (2000)

THE EUROPEAN
PHYSICAL JOURNAL B
EDP Sciences

Studies of the exactly dimerized bilayer Heisenberg model via strong coupling expansions

Q. Gu[1,a] and J.L. Shen[2]

[1] Center for Advanced Study, Tsinghua University, Beijing 100084, PR China
[2] Institute of Physics, Chinese Academy of Sciences, Beijing 100080, PR China

Received 16 March 2000 and Received in final form 2 July 2000

Abstract. The one-triplet excitation spectra and thermodynamic properties for the dimerized phase of the frustrated bilayer Heisenberg model are studied using strong-coupling expansion theory. The model has an exact dimerized ground state as well as exact one-triplet excitations in a special case that the frustration J_2 is equal to the in-plane coupling J_1. We demonstrate that the models with and without frustrations have distinct excitation spectra, so their thermodynamic properties exhibit quite different behaviors. Especially, the low-temperature behaviors of the frustrated model with $J_1 = J_2$ are independent of the inter-dimer couplings, due to the exact one-triplet excitations.

PACS. 75.10.Jm Quantized spin models – 75.30.Kz Magnetic phase boundaries (including magnetic transitions, metamagnetism, etc.) – 75.40.Cx Static properties (order parameter, static susceptibility, heat capacities, critical exponents, etc.)

In the recent past few years, the bilayer Heisenberg model on a square lattice has been intensively studied [1–5]. This model is introduced to explain the unusual normal state properties of the high temperature superconductor $YBa_2Cu_3O_{6+x}$ firstly [1], but it has more theoretical interest in its own right for it displays a *continuous* quantum phase transition as the interlayer coupling J_0 becomes strong. The model with weak J_0 has a Néel ordered ground state. With J_0 increasing, the interlayer coupling destroys the long-range order and leads to the dimerization of each pair of spins connected by J_0. The transition point has been determined to be $J_{1c} \approx 0.4\,J_0$ [3,4] where J_1 is the in-plane coupling. The excitations are spin-triplets with a finite gap. The dimerized phase with gapped excitations has been observed in the strong-coupling bilayer compound $BaCuSi_2O_6$ [6].

In this paper, we study a frustrated bilayer Heisenberg model (FBM) which shows richer ground state properties [7]. As indicated in Figure 1, this model is defined on a double layers which connect to each other not only perpendicularly by J_0, but also diagonally by J_2. The Hamiltonian is written as $H = H^0 + H^{\mathrm{I}}$, with

$$\begin{aligned} H^0 &= \sum_i [J_0 \mathbf{S}_{1,i} \cdot \mathbf{S}_{2,i} - h(S^z_{1,i} + S^z_{2,i})], \\ H^{\mathrm{I}} &= \sum_{\langle ij \rangle} [J_1(\mathbf{S}_{1,i} \cdot \mathbf{S}_{1,j} + \mathbf{S}_{2,i} \cdot \mathbf{S}_{2,j}) \\ &\quad + J_2(\mathbf{S}_{1,i} \cdot \mathbf{S}_{2,j} + \mathbf{S}_{2,i} \cdot \mathbf{S}_{1,j})], \end{aligned} \tag{1}$$

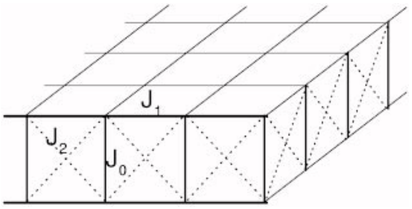

Fig. 1. The frustrated bilayer model with $2N$ spins. The two thick parallel lines in the front of the figure denote the frustrated spin-ladder.

and $J_0, J_1, J_2 > 0$. H^0 describes a isolated dimer system and H^{I} represents interactions between the dimers. h is the external magnetic field. It has been found that the FBM has an exactly dimerized ground state as well as a class of exact excited states when the couplings satisfy the constraint $J_1 = J_2 = J$ and J is smaller than a critical value J_c [7]. At $J_c \approx 0.43J_0$, the FBM undergoes a disorder-order phase transition. But, the transition is different from that occurring in the non-frustrated model. (i) In FBM the transition is *first-order*, while it is *second-order* in the non-frustrated model. (ii) When $J > J_c$, the FBM has *spin-1* Néel order, *i.e.*, the two spins connected by J_0 form spin triplets. In contrast, the non-frustrated model with large J_1 has *spin-*$\frac{1}{2}$ Néel order.

Figure 2 shows the schematic phase diagram of the FBM in the parameter space (J_1, J_2). The present study is focused on the dimerized phase. In the dimerized phase, the coupling J_0 is stronger than J_1 and J_2, so we can treat H^{I} as a perturbation and perform a strong-coupling

---

[a] e-mail: `qgu@castu.phys.tsinghua.edu.cn`

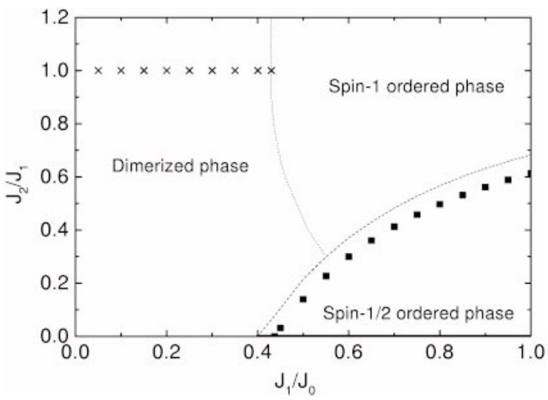

Fig. 2. Schematic phase diagram of the frustrated bilayer model.

expansion. Eigenstates of the unperturbed term H^0 are direct products of the eigenstates of each spin-pair whose Hamiltonian is $H_i^0 = J_0 \mathbf{S}_{1,i} \cdot \mathbf{S}_{2,i} - h(S_{1,i}^z + S_{2,i}^z)$. The two coupled spins $\mathbf{S}_{1,i}$ and $\mathbf{S}_{2,i}$ form four eigenstates including a singlet state $|s_i\rangle$ with eigenvalue $E_s = -3J_0/4$ and three triplet states $|t_i^\sigma\rangle$ with eigenvalues $E_t^\sigma = J_0/4 - \sigma h$, corresponding to the spin-z component $\sigma = S_{1,i}^z + S_{2,i}^z = -1, 0, 1$. Therefore, the ground state of H^0 is $|g\rangle = |s...s...s\rangle$, and the nth excited eigenstates $|n\rangle$ are obtained by promoting n site-singlets to triplets and leaving $(N-n)$ sites in singlets.

Earlier than the FBM, a frustrated two-leg spin-ladder had attracted much attention [8–11]. As shown in Figure 1, the model can be regard as a special case of the FBM. Bose and Gayen firstly suggested that the frustrated two-leg spin-ladder has completely dimerized ground state in the case of $J_1 = J_2$ [8]. It undergoes a first-order transition from the dimerized phase to the Haldane-type phase as J_1 increases. The phase diagram in a larger parameter space (J_1, J_2) has studied by Zheng *et al.* [11]. Due to the similarity between the two models, present treatment of the FBM is also suitable to the frustrated spin-ladder.

Firstly, performing a third-order zero-temperature perturbation expansion [12,13], we obtain the ground state energy,

$$E_{\mathrm{G}} = -\frac{3J_0}{4}N - \frac{3A^2}{J_0}N - \frac{3A^2B}{J_0^2}N. \tag{2}$$

Here, A and B are coupling constants, $A = (J_1 - J_2)/2$ and $B = (J_1 + J_2)/2$. N is the number of the sites on each layer. Next, we look at the first excited state $|s...t^\sigma...s\rangle$ (which represents the one-triplet excitations). The unperturbed first excited state is expressed as the Bloch state:

$$|1_{\mathbf{k}}^\sigma\rangle = \frac{1}{\sqrt{N}} \sum_i \mathrm{e}^{\mathrm{i}\mathbf{k}\mathbf{r}_i} |s...t_i^\sigma...s\rangle, \tag{3}$$

where $\mathbf{k}$ is the wave vector in the first Brillouin zone. The corrected excitation spectrum up to the third-order expansion is given by

$$\begin{aligned}
\omega_t^\sigma(\mathbf{k}) = {} & J_0 + 2A(\cos k_x + \cos k_y) + 6\frac{A^2}{J_0} \\
& - \frac{A^2}{J_0}(\cos 2k_x + \cos 2k_y) - 2\frac{A^2}{J_0}\Big[\cos(k_x + k_y) \\
& + \cos(k_x - k_y)\Big] + 6\frac{A^2B}{J_0^2} - 4\frac{A^3}{J_0^2}(\cos k_x + \cos k_y) \\
& - 2\frac{A^2B}{J_0^2}(\cos 2k_x + \cos 2k_y) - 4\frac{A^2B}{J_0^2}\Big[\cos(k_x + k_y) \\
& + \cos(k_x - k_y)\Big] + \frac{A^3}{J_0^2}(\cos 3k_x + \cos 3k_y) \\
& + 3\frac{A^3}{J_0^2}\Big[\cos(2k_x + k_y) + \cos(2k_x - k_y) \\
& + \cos(k_x + 2k_y) + \cos(k_x - 2k_y)\Big].
\end{aligned} \tag{4}$$

Because of the existence of the inter-dimer couplings J_1 and J_2, the excitation energy is expanded to a continuous energy band with bandwidth $w \approx 4|J_1 - J_2|$. The spectrum opens a energy gap at $\mathbf{k} = (\pi, \pi)$,

$$\Delta = \omega_t^\sigma(\pi, \pi) = J_0 - 4A - \frac{6A^2B}{J_0^2} - \frac{6A^3}{J_0^2} \cdot \tag{5}$$

In the parameter space (J_1, J_2), there are two cases which are of special interest. One is that $J_2 = 0$, when the model is reduced to the non-frustrated bilayer model. Another is that $J_2 = J_1$, when the FBM has exactly dimerized ground state, $|g\rangle = |s...s\rangle$. In the former case, Δ decreases with J_1 and vanishes at $J_1\mathrm{c} \approx 0.437J_0$ which signals a second-order phase transition from the dimerized phase to the spin-$\frac{1}{2}$ Néel phase. The critical value is in good agreement with the numerical result [3,4]. For small J_2, the phase boundary is similarly determined by examining the disappearance of the gap. The result is shown in Figure 2 as solid squares. For larger J_2, the phase transition is of first-order and the gap will not disappear continuously at the critical point. In order to determine the phase boundary, one need compare the ground state energy of the two phases. The ground state energy of the dimerized phase becomes larger with J_2 increasing (see Eq. (2)). Unfortunately, the present method can not calculate E_{G} of the ordered phase.

$J_2 = J_1$ is a very special point. At this point, all the correction terms in equations (2, 4) are cancelled. The ground state energy, $E_{\mathrm{G}} = -3J_0N/4$, and the excitation spectrum, $\omega_t^\sigma = J_0$, are equal to those of the unperturbed state $|g\rangle$ and $|1_{\mathbf{k}}^\sigma\rangle$ respectively. Those results are consistent with the conclusion that the FBM with $J_2 = J_1$ has *exact* ground state and first-excited state [7,9]. Note that the first-excitation spectrum is dispersionless and independent of the inter-dimer couplings. In the following, we investigate thermodynamic properties of the FBM at the special point. Henceforth, it is assumed that $J_2 = J_1 = J$ for the FBM.

The thermodynamic properties are studied by a third-order cumulant expansion method. This method is well

$$
\begin{aligned}
F(h,T) = {} & -\frac{3J_0}{4}N - \frac{1}{\beta}N\ln E + \left[B\mathrm{e}^{-2\beta J_0}(\mathrm{e}^{2\beta h}+\mathrm{e}^{-2\beta h}-2) - \frac{3A^2}{2J_0}(1-\mathrm{e}^{-2\beta J_0}) - \frac{3A^2B}{2J_0^2}(1-\mathrm{e}^{-2\beta J_0})\right.\\
& \left. -A^2\beta\mathrm{e}^{-\beta J_0}(\mathrm{e}^{\beta h}+\mathrm{e}^{-\beta h}+1) - \frac{B^2\beta}{2}\mathrm{e}^{-2\beta J_0}(\mathrm{e}^{2\beta h}+\mathrm{e}^{-2\beta h}+2\mathrm{e}^{\beta h}+2\mathrm{e}^{-\beta h}+6) + \frac{3A^2B\beta}{J_0}\mathrm{e}^{-2\beta J_0} + \frac{B^3\beta^2}{6}\mathrm{e}^{-2\beta J_0}(\mathrm{e}^{2\beta h}+\mathrm{e}^{-2\beta h}-8)\right]2NE^{-2}\\
& -\left[B^2\beta\mathrm{e}^{-3\beta J_0}(\mathrm{e}^{3\beta h}+\mathrm{e}^{-3\beta h}-\mathrm{e}^{\beta h}-\mathrm{e}^{-\beta h}) - A^2B\beta^2\mathrm{e}^{-2\beta J_0}(\mathrm{e}^{2\beta h}+\mathrm{e}^{-2\beta h}-2) - B^3\beta^2\mathrm{e}^{-3\beta J_0}(\mathrm{e}^{\beta h}+\mathrm{e}^{-\beta h}+1)(\mathrm{e}^{2\beta h}+\mathrm{e}^{-2\beta h}-2)\right]6NE^{-3}\\
& + \left[B^2\beta\mathrm{e}^{-4\beta J_0}(\mathrm{e}^{2\beta h}+\mathrm{e}^{-2\beta h}-2) - \frac{3A^2B\beta}{J_0}(\mathrm{e}^{-2\beta J_0}-\mathrm{e}^{-4\beta J_0}) - 2A^2B\beta^2\mathrm{e}^{-3\beta J_0}(\mathrm{e}^{\beta h}+\mathrm{e}^{-\beta h}+1) - B^3\beta^2\mathrm{e}^{-4\beta J_0}(\mathrm{e}^{2\beta h}+\mathrm{e}^{-2\beta h}\right.\\
& \left. +2\mathrm{e}^{\beta h}+2\mathrm{e}^{-\beta h}+6)\right](\mathrm{e}^{2\beta h}+\mathrm{e}^{-2\beta h}-2)7NE^{-4} + 18B^3\beta^2\mathrm{e}^{-4\beta J_0}(\mathrm{e}^{4\beta h}+\mathrm{e}^{-4\beta h}-2)NE^{-4} - 60B^3\beta^2\mathrm{e}^{-5\beta J_0}(\mathrm{e}^{2\beta h}+\mathrm{e}^{-2\beta h}-2)\\
& \times(\mathrm{e}^{3\beta h}+\mathrm{e}^{-3\beta h}-\mathrm{e}^{\beta h}-\mathrm{e}^{-\beta h})NE^{-5} + \frac{116}{3}B^3\beta^2\mathrm{e}^{-6\beta J_0}(\mathrm{e}^{2\beta h}+\mathrm{e}^{-2\beta h}-2)^3NE^{-6}, \qquad (9)
\end{aligned}
$$

---

applicable to the dimerized phase [14]. First of all, we calculate the partition function, $Z = \mathrm{Tr}[\exp(-\beta H)]$, whose cumulant expansion is

$$Z = Z_0 \exp\left[\sum_{n=1}^{\infty} U_n\right]. \qquad (6)$$

The former three cluster functions U_n are defined as

$$
\begin{aligned}
U_1 &= \frac{Z_1}{Z_0},\\
U_2 &= \frac{Z_2}{Z_0} - \frac{1}{2}\left(\frac{Z_1}{Z_0}\right)^2,\\
U_3 &= \frac{Z_3}{Z_0} - \frac{Z_2Z_1}{Z_0^2} + \frac{1}{3}\left(\frac{Z_1}{Z_0}\right)^3. \qquad (7)
\end{aligned}
$$

Here Z_n $(n = 0, 1, 2, 3)$ is the nth order perturbation expansion,

$$
\begin{aligned}
Z_n = {} & (-1)^n \int_0^\beta \mathrm{d}\tau_1\\
& \times \int_0^{\tau_1} \mathrm{d}\tau_2 \ldots \int_0^{\tau_{n-1}} \mathrm{d}\tau_n \mathrm{Tr}[\mathrm{e}^{-\beta H^0} H^{\mathrm{I}}(\tau_1)H^{\mathrm{I}}(\tau_2)\ldots H^{\mathrm{I}}(\tau_n)], \qquad (8)
\end{aligned}
$$

with $H^{\mathrm{I}}(\tau) = \mathrm{e}^{\tau H^0}H^{\mathrm{I}}\mathrm{e}^{-\tau H^0}$ and $\beta = \frac{1}{k_{\mathrm{B}}T}$. Z_n can be integrated based on the eigenstates of the unperturbed Hamiltonian H^0 [14] and then we obtain the cumulant expansion of the free energy from the partition function $F(h,T) = -\frac{1}{\beta}\ln Z$,

see equation (9) above

where $E = 1 + (1 + \mathrm{e}^{\beta h} + \mathrm{e}^{-\beta h})\mathrm{e}^{-\beta J_0}$. The specific heat $C(T)$ and the uniform susceptibility $\chi(T)$ per spin can be derived from the free energy by the standard method.

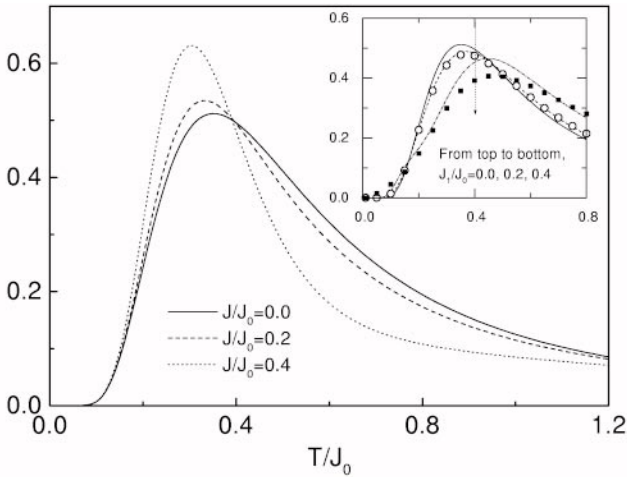

Fig. 3. Specific heat per spin $C(T)$ of the FBM *versus* temperature T for $J/J_0 = 0.0$, 0.2, 0.4. The inset shows the specific heat for the non-frustrated bilayer model. Lines show results of the cumulant expansions and symbols are obtained by equation (10).

Figure 3 shows the specific heat of the FBM with $J/J_0 = 0.0$, 0.2 and 0.4. To make a comparison, $C(T)$ of the non-frustrated bilayer model is plotted in the inset. Both the two models show a round peak in the specific heat, which is a basic feature of the dimerized phase. Furthermore, some different behaviors are observed. (1) At low temperatures, the specific heat of the FBM seems independent of the inter-dimer coupling J. But the low-temperature behaviors of the non-frustrated model vary with J_1. (2) At higher temperatures, for the FBM the peak grows and sharpens as J becomes strong. The position of the peak moves left gradually. For the latter model, in contrast, the peak becomes low and round and move right with J_1 increasing.

The low temperature behaviors are determined by the first excitations. According to equation (4), it is easy to understand the low temperature behaviors of the two models because the excitation spectrum of the FBM is independent of J while the excitation spectrum of the non-frustrated model depends strongly on J_1, with bandwidth $w \approx 4J_1$.

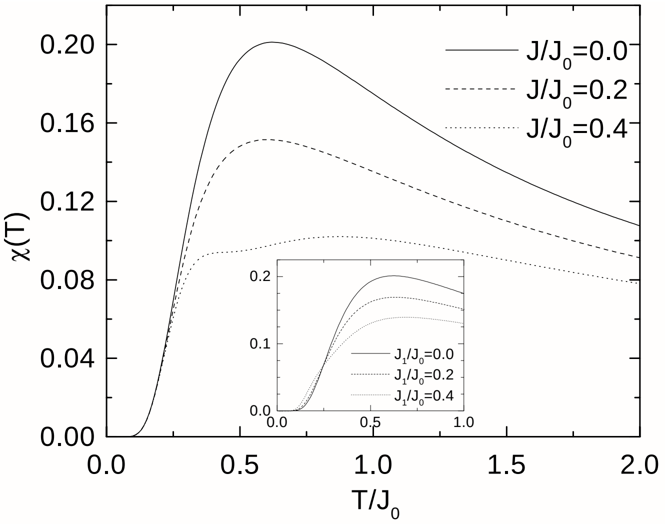

Fig. 4. Uniform susceptibility per spin $\chi(T)$ of the FBM for $J/J_0 = 0.0, 0.2, 0.4$, compared with those of the non-frustrated model shown in the inset.

For the non-frustrated model, reference [15] provided a simple method to estimate the specific heat using the first excitation spectrum,

$$C(T) = \frac{3}{2}\beta^2 \frac{z''(\beta)}{1+3z(\beta)} - \frac{9}{2}\beta^2 \left(\frac{z'(\beta)}{1+3z(\beta)}\right)^2 . \qquad (10)$$

Here $z(\beta) = \int_{\mathrm{BZ}} \mathrm{d}\mathbf{k} \mathrm{e}^{-\beta\omega_t^{\sigma}(\mathbf{k})}/\Omega^*$, Ω^* is the area of the Brillouin zone. $z'(\beta)$ and $z''(\beta)$ are the first- and second-order derivations of $z(\beta)$ with respect to β. They argued that the estimate is reliable both at low and high temperatures [15]. Substitute equation (4) into (10), we find that the obtained results (shown in the inset as symbols) display a peak varying with J_1 in the same way as the cumulant expansion results although they are not in quantitative agreement. Contrarily, for the FBM the first excited state does not account for the J-dependence of $C(T)$ at high temperatures since $\omega_t^{\sigma}(\mathbf{k})$ is a *constant* for different J. In this case, one must take the higher excited states (which represent multi-triplet excitations) into account because the multi-triplet excitations become the favorable excitations at higher temperatures. For example, the excited energy of the two-triplet excitation [7] $|T\rangle = |s...(t_i^0 t_{i+1}^0 - t_i^1 t_{i+1}^{-1} - t_i^{-1} t_{i+1}^1)...s\rangle$ is $\omega_T = 2J_0 - 2J$ which is obviously lower than that of two separate triplets. The energy of each triplet averages $J_0 - J$. Using this average excitation energy to estimate the specific heat approximately by equation (10), we can obtain the peak in $C(T)$ sharpening and moving left with J. It explains the cumulant expansion result qualitatively. Therefore, we may draw a conclusion that dominant contributions to the high-temperature properties come from the multi-triplet excitations.

The uniform susceptibility $\chi(T)$ of the FBM is plotted in Figure 4, compared with those of the non-frustrated model shown in the inset. The low-temperature behaviors of $\chi(T)$ are determined by the lowest spin-flip excitation $|t_i^{\sigma}\rangle$, so it is no wonder that $\chi(T)$ of the FBM displays similar low temperature behaviors for different J. At higher temperatures, $\chi(T)$ of the FBM is smaller than the corresponding value of the non-frustrated model. It might be relative to the fact that $|T\rangle$ is a spinless excitation and therefore it has no contributions to $\chi(T)$.

One can also get the internal energy $U(T)$ from equation (9). As $T \to 0$, $U(T)$ tends to the ground state energy E_{G} as described by equation (2) which is correct only in the dimerized phase. Therefore, the cumulant expansion method is not suitable to calculated thermodynamics, especially the low temperature behaviors, of the ordered phase. As a consequence, the obtained results become not quite reliable with the coupling J close to the critical point J_{c}. It can be seen that there appears a shoulder in $\chi(T)$ at $J/J_0 = 0.4$. When $J > J_{\mathrm{c}}$, the shoulder will protrude.

To summarize, we have performed third-order cumulant expansions to study thermodynamic properties of the frustrated bilayer model in the dimerized phase. The one-triplet excitation spectrum is also calculated by a third-order zero-temperature perturbation theory. The models with and without frustrations have distinct excitation spectra, so their thermodynamic properties exhibit quite different behaviors. Especially, the low-temperature behaviors of the frustrated bilayer model are independent of the inter-dimer couplings. We demonstrate that the one-triplet excitation spectrum can qualitatively account for the thermodynamics of the non-frustrated model both at low and high temperatures, while in the frustrated model the high temperature behaviors are apparently affected by the multi-triplet excitations. Our study also suggest that the strong coupling expansions yield reasonable results at the whole temperature region for the dimerized phase.

References

1. A.J. Millis, H. Monien, Phys. Rev. Lett. **70**, 2810 (1993); Phys. Rev. B **50**, 16606 (1994).
2. A.V. Chubukov, D.K. Morr, Phys. Rev. B **52**, 3521 (1995).
3. A.W. Sandvik, D.J. Scalapino, Phys. Rev. Lett. **72**, 2777 (1994).
4. M.P. Gelfand, Phys. Rev. B **53**, 11309 (1996).
5. N. Elstner, R.R.P. Singh, Phys. Rev. B **57**, 7740 (1998).
6. Y. Sasago, K. Uchinokura, A. Zheludev, G. Shirane, Phys. Rev. B **55**, 8357 (1997).
7. H.Q. Lin, J.L. Shen, J. Phys. Soc. Jpn **69**, 878 (2000).
8. I. Bose, S. Gayen, Phys. Rev. B **48**, 10653 (1993).
9. Y. Xian, Phys. Rev. B **52**, 12485 (1995).
10. A.K. Kolezhuk, H.-J. Mikeska, Phys. Rev. B **56**, r11380 (1997).
11. Zheng Weihong, V. Kotov, J. Oitmaa, Phys. Rev. B **57**, 11439 (1998).
12. T. Barnes, E. Dagotto, J. Riera, E. Swanson, Phys. Rev. B **47**, 3196 (1993).
13. M. Reigrotzki, H. Tsunetsugu, T.M. Rice, J. Phys. Cond. Matt. **6**, 9235 (1994).
14. Q. Gu, J.L. Shen, Phys. Lett. A **251**, 150 (1999).
15. M. Troyer, H. Tsunetsugu, D. Würtz, Phys. Rev. B **50**, 13515 (1994).